DOI: 10.19884/j.1672-5220.202412018

Radiation-Grafted PBT Biomaterials for Enhanced Uric Acid Adsorption and Blood Compatibility

MO Yaoxiang[1], LI Chun[1], WANG Siqi[1], XUE Jiahe[1], SHEN Li[1], WANG Hengdong[2*], CHEN Qianjin[1*]
1. College of Chemistry and Chemical Engineering, Donghua University, Shanghai 201620, China
2. Shanghai Institute of Applied Physics, Chinese Academy of Sciences, Shanghai 201821, China

Abstract: The efficient removal of uric acid from blood via purification is a novel approach for the treatment of gout and hyperuricemia. In this study, a new polybutylene terephthalate (PBT) biomembrane with good uric acid adsorption capacity and desirable blood compatibility was prepared via radiation grafting of *N*-(4-vinylcarbonyloxyphenyl) acetamide (NVA) and acrylic acid (AA). The chemical structure and surface morphology of the modified membrane were characterized by Fourier transform infrared (FTIR) spectroscopy, X-ray photoelectron spectroscopy (XPS), and scanning electron microscopy (SEM). The wettability of the modified membrane was determined by measuring the water contact angle and water absorption rate. The results indicated that the modified membrane exhibited a maximum uric acid adsorption rate of (6.80±0.20)% with minimal impact on blood cell counts. This study provides a promising strategy for developing safe and efficient biomaterials for the treatment of gout and hyperuricemia.

Keywords: uric acid adsorption; radiation grafting; polybutylene terephthalate (PBT); *N*-(4-vinylcarbonyloxyphenyl) acetamide (NVA); blood cell count
CLC number: R457.1 **Document code**: A
Article ID: 1672-5220(2026)04-0001-12

0 Introduction

With the changes in lifestyle and excessive intake of purine-containing foods, the prevalence of gout and hyperuricemia has been rising annually, and these diseases have become a major global public health challenge[1-3]. Although remarkable progress has been achieved in gout therapy, long-term administration of both conventional and novel drugs still induces unavoidable side effects[4-5]. For instance, probenecid increases the risk of kidney stones, and benzbromarone has notable hepatotoxicity. Moreover, prolonged use of these drugs can lead to resistance, limiting their clinical application[6]. Therefore, developing more straightforward and efficient methods for uric acid removal is crucial for gout treatment.

Hemodialysis is regarded as the most promising method[7-11]. Polybutylene terephthalate (PBT) nonwoven fabrics have been extensively adopted for medical consumables and blood filtration, owing to their ultrafine fibers, small effective pore size, and low manufacturing cost[12-13]. However, the pristine PBT material has poor hydrophilicity, which restricts its interaction with aqueous solutions, such as blood[14]. Therefore, improving the hydrophilicity and uric acid filtration-adsorption performance of PBT materials via surface modification, shortening blood filtration time, and boosting filtration-adsorption efficiency have become a key research focus[15-16].

Radiation grafting has attracted great attention due to its simplicity, being free of initiators, and the capability to be performed at room temperature[17-18]. Zhong et al.[19] used ultraviolet (UV) radiation to graft —COOH and zwitterionic groups onto the PBT surface. The modified material exhibited excellent platelet compatibility. Heller et al.[20] enhanced the protein adsorption and ion exchange efficiency by grafting glycidyl methacrylate (GMA) onto the PBT surface through UV radiation. Salvagnini et al.[21] modified PBT using UV radiation to functionalize its surface. By coupling cell adhesion molecules such as the glycyl-arginyl-glycyl-aspartyl-serine (GRGDS) peptide, they effectively enhanced leukocyte capture efficiency.

There are numerous studies focused on platelet and leukocyte filtration materials. However, studies on uric acid filtration and adsorption remain limited. Therefore, acetaminophen (*N*-acetyl-*p*-aminophenol, APAP, Ac—NH—C_6H_4—OH, where Ac represents the acetyl group CH_3CO—) was selected as a grafting monomer to modify the PBT membrane in this study. The amide group and benzene ring of APAP can form hydrogen bonds and π-π interactions with uric acid, respectively, thereby enhancing the uric acid adsorption capacity of PBT[22-24]. Preliminary studies showed that it was difficult to directly graft APAP onto the PBT membrane. Therefore, in this study, *N*-(4-vinylcarbonyloxyphenyl) acetamide (NVA) was synthesized through the

Received date: 2024-12-30
* Correspondence should be addressed to WANG Hengdong, email: wanghd99@sina.com; CHEN Qianjin, email: qianjinchen@dhu.edu.cn
Citation: Mo Y X, Li C, Wang S Q, et al. Radiation-grafted PBT biomaterials for enhanced uric acid adsorption and blood compatibility[J]. *Journal of Donghua University (English Edition)*, 2026, 43(4): 1-12.

esterification of APAP with acryloyl chloride, and its highly reactive vinyl structure was utilized for subsequent radiation grafting. As illustrated in Fig. 1, the process involves radiation grafting of NVA and acrylic acid (AA) onto the surface of the PBT membrane. The as-prepared membrane is denoted as PBT-NVA-AA. The blood compatibility of this membrane was also preliminarily explored. This study provides new material options and potential clinical applications for the treatment of gout and hyperuricemia.

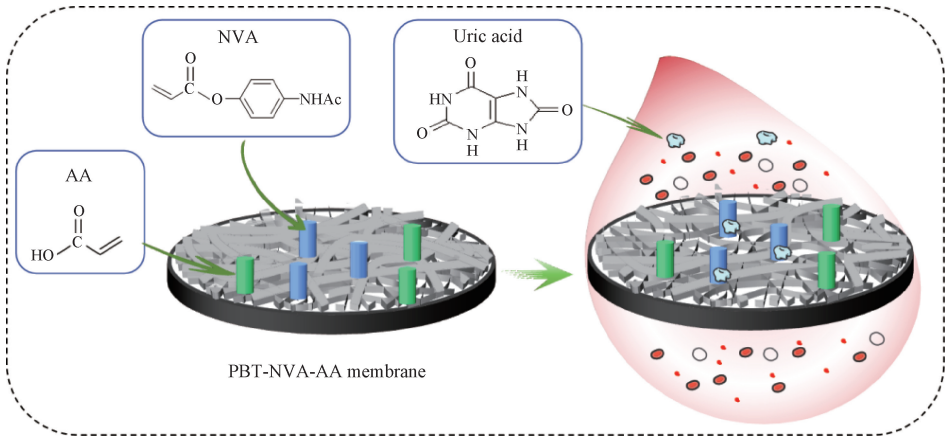


Fig. 1 Schematic of PBT-NVA-AA membrane for uric acid removal during blood filtration

1 Materials and Methods

This study was approved by the Research Ethics Committee of Donghua University (SRSY202406240030) and conducted in accordance with the approved protocol and informed consent forms.

1.1 Materials and reagents

The PBT membrane with a specification of 45B and dimensions of 60.0 cm × 30.0 cm × 1.2 mm was purchased from Shanghai Shilong Technology Co., Ltd., China. AA, NaOH, CH_2Cl_2, glucose, NaCl, APAP, thionyl chloride ($SOCl_2$) and pyridine (Py) were purchased from Shanghai Macklin Biochemical Technology Co., Ltd., China. Copper acetate was purchased from Shanghai Lingfeng Chemical Reagent Co., Ltd., China. All chemicals were of analytical grade. The ^{60}Co-γ radiation source used for grafting was provided by the Shanghai Institute of Applied Physics, Chinese Academy of Sciences, with a radioactivity of 5.957×10^{15} Bq. Whole blood (with blood preservation solution Ⅲ) was collected from healthy volunteers on the same day and provided by the Chengdu Blood Center, China.

1.2 Preparation of PBT-NVA-AA membrane

1.2.1 Synthesis of NVA

NVA was synthesized following the method outlined in Refs. [25–26]. The synthesis route of NVA is shown in Fig. 2. First, acryloyl chloride was prepared via the reaction of AA with $SOCl_2$ in the presence of Py at 65 ℃ under reflux, followed by vacuum distillation to afford pure acryloyl chloride. Second, APAP was converted into its sodium phenoxide precursor by treatment with aqueous NaOH at 10 ℃. Thereafter, the as-prepared sodium phenoxide reacted with acryloyl chloride at 20 – 25 ℃ under basic conditions. The resulting mixture was then washed and purified with CH_2Cl_2, and the target NVA product was collected as a white crystalline solid with an isolated yield of 43.1%.

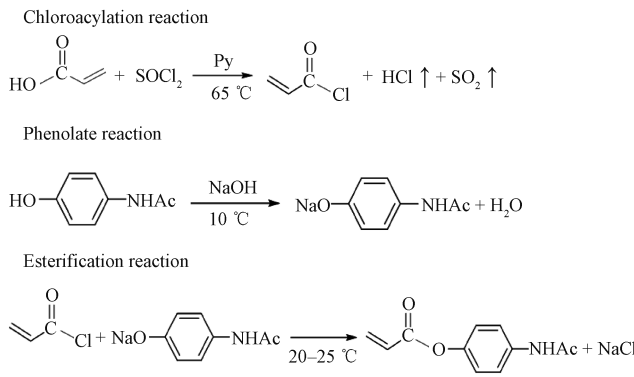


Fig. 2 Synthesis route of NVA

1.2.2 Preparation of PBT-NVA-AA membrane by radiation modification

The preparation process of the PBT-NVA-AA membrane is illustrated in Fig. 3.

The PBT membrane was cut into a square of 10 cm × 10 cm and then treated with ultrasound in acetone, ethanol, and ultrapure water for 10 min each, followed by drying at 50 ℃ until a constant mass was reached.

The pre-treated PBT membrane was placed in an irradiation tube. NVA (1.2 g) was dissolved in a 60 mL mixture solution of deionized water and ethanol (a volume ratio of 1∶1). After vacuuming and nitrogen gas introduction, the sealed irradiation tube was exposed to ^{60}Co-γ radiation at a dose of 10 kGy for 24 h. After the reaction, the membrane was washed sequentially with acetone and deionized water to remove residual monomers and homopolymers, then dried at 50 ℃ under vacuum. The product was named PBT-NVA membrane. The

grafting degree of NVA was calculated as

$$D_{gN} = (m_{gN} - m_0) / m_0, \quad (1)$$

where D_{gN} represents the grafting degree of NVA; m_0 represents the membrane mass before grafting; m_{gN} represents the membrane mass after grafting of NVA.

The PBT-NVA membrane was placed in an irradiation tube, 3 mL AA and 0.003 g copper acetate (an anti-polymerization agent) were added to 60 mL deionized water, and nitrogen gas was introduced. The mixture was sealed and irradiated with 10 kGy for 24 h using ^{60}Co-γ radiation. The membrane was cleaned, and the product, named PBT-NVA-AA membrane, was obtained. The grafting degree of AA was calculated as

$$D_{gA} = (m_{gA} - m_{gN}) / m_{gN}, \quad (2)$$

where D_{gA} represents the grafting degree of AA; m_{gA} represents the membrane mass after grafting of AA.

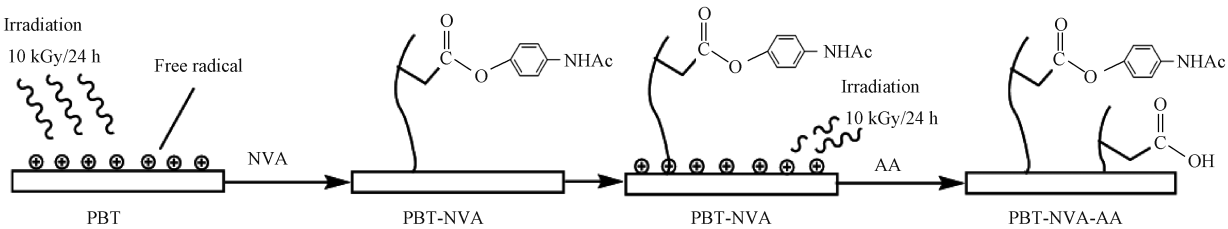


Fig. 3 Preparation process of PBT-NVA-AA membrane

1.3 Characterization

Proton nuclear magnetic resonance (^{1}H NMR) and high-resolution mass spectrometry (HRMS) spectra of the product were analyzed using an NMR spectrometer (Bruker AVANCE Ⅲ HD 600 MHz, Bruker, Switzerland) and a high-resolution mass spectrometer (Xevo G2-XS QTof, Waters, USA), respectively. Fourier transform infrared (FTIR) spectroscopy was performed on a spectrometer (DA7440GP, Swedish Perten, Sweden). X-ray photoelectron spectroscopy (XPS) measurements were carried out on an XPS spectrometer (K-Alpha, Thermo Fisher Scientific, USA), and the C1s characteristic peak was referenced at 284.8 eV for charge calibration. Surface morphology of the membrane was characterized via a scanning electron microscope (S-4800, Hitachi Ltd., Japan). The membrane surface water contact angle was determined using an optical contact angle goniometer (Theta Lite, Biolin Scientific, Finland). Water absorption was measured according to the standard GB/T 21655.1—2023 Textiles—evaluation of absorption and quick-drying—part 1: method for combination tests. The water absorption rate W was calculated as

$$W = (m_w - m_1) / m_1, \quad (3)$$

where m_1 represents the membrane mass before water absorption; m_w represents the membrane mass after water absorption.

Uric acid concentration was measured using test kits (Shanghai Enzyme-linked Biotechnology Co., Ltd., China) with a UV-visible spectrophotometer at 505 nm and 37 ℃ for 30 min. All experiments were repeated three times to ensure reproducibility. The standard deviation (SD) was calculated for each set of measurements to assess the precision of the results. Experimental error analysis was conducted, and the data were reported as the mean±SD.

1.4 Adsorption experiments

1.4.1 Uric acid adsorption performance

PBT-NVA-AA membrane samples were cut into discs with a diameter of 2 cm and loaded into blood filters to serve as filter media. Uric acid solution (4 mL) of varying concentrations (containing a mass fraction of 0.9% NaCl and 0.1% glucose to simulate blood viscosity) was added to the filter, and the solution was filtered under normal pressure into reagent tubes. The uric acid concentration in the filtered solution was measured.

1.4.2 Adsorption isotherm

Identical PBT-NVA-AA membrane samples (D_{gN} = 8%, D_{gA} = 15%, each size of 10 cm × 10 cm) were added to different uric acid solutions ranging from 200 to 400 μmol/L and adsorbed at room temperature for 24 h. The concentration of uric acid in the residual solution was measured after membrane removal. The adsorption isotherms were fitted using the Langmuir isotherm model (Eq. (4)) and the Freundlich isotherm model (Eq. (5))[15]:

$$Q_e = (Q_m K_L C_e) / (1 + K_L C_e), \quad (4)$$

$$Q_e = K_F C_e^{\frac{1}{n}}, \quad (5)$$

where Q_e is the equilibrium adsorption amount; Q_m is the maximum adsorption capacity; K_L is the Langmuir constant; C_e is the equilibrium concentration; K_F is the Freundlich constant; n is the adsorption intensity index reflecting the uniformity of adsorption sites on the surface.

1.5 Blood cell count

PBT-NVA-AA membrane samples were cut into discs with a diameter of 2 cm and loaded into blood filters to serve as filter media. The blood sample (4 mL) was added to the filter, and the solution was filtered under normal pressure into reagent tubes. A fully automatic hematology analyzer (XS-500i, Sysmex Corporation,

Japan) was used to measure the effect of the PBT-NVA-AA membrane on blood cell counts after filtration.

1.6 Statistical analysis

To assess the reliability and reproducibility of the experimental results, all adsorption experiments were performed in triplicate, and the data were presented as mean ± SD. All analyses were performed using Origin 2022 software.

2 Results and Discussion

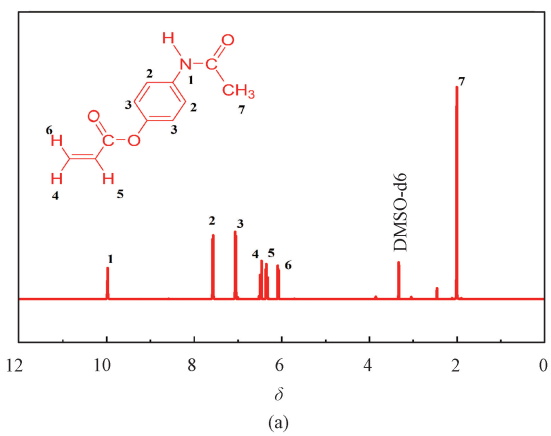
2.1 Physicochemical characteristics of PBT-NVA-AA membrane

The ^{1}H NMR spectrum of NVA synthesized through the esterification of acryloyl chloride with APAP is shown in Fig. 4(a). The chemical shift δ = 9.98 corresponds to the hydrogen in the amide group of the acetamide group (H-1); δ = 7.60 corresponds to two hydrogens on the aromatic ring near the acetamide group (H-2); δ = 7.09 corresponds to two hydrogens on the aromatic ring near the ester carbonyl (H-3); δ = 6.47 corresponds to one hydrogen on the vinyl group (H-4); δ = 6.35 corresponds to another hydrogen on the vinyl group (H-6); δ = 6.08 corresponds to the hydrogen on the vinyl group adjacent to the carbonyl (H-5); δ = 2.01 corresponds to the three hydrogens on the methyl group (H-7). The integral ratio of these seven groups of hydrogens is calculated as 1∶2∶2∶1∶1∶1∶3.

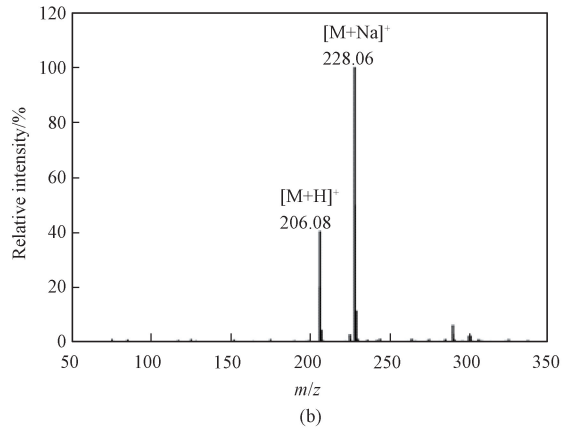
The HRMS spectrum of NVA (Fig. 4(b)) reveals a $[M+Na]^+$ peak at a mass-to-charge ratio m/z of 228.06, which is in excellent agreement with the theoretical value. This high level of precision confidently establishes the molecular formula of the compound as $C_{11}H_{11}NO_3$, corresponding to a relative molecular mass of approximately 205. Furthermore, the calculated degree of unsaturation (DBE) is 7, which aligns well with the expected number of double bonds, aromatic rings, ester, and amide functionalities within the molecular structure. The HRMS data further support the purity and identity of NVA.

As shown in Fig. 4(c), compared with untreated PBT, the PBT-NVA-AA membrane exhibits a weak broad peak around 3 300 cm^{-1}, which may be assigned to N—H stretching vibrations in APAP[27-28]. The peak around 3 000 cm^{-1} decreases, possibly due to the introduction of —COOH groups on the PBT surface, affecting the relative peak intensity. The peaks at 1 550 and 1 610 cm^{-1} are enhanced compared with untreated PBT, indicating the presence of N—H bending vibration[29]. The absorption at 1 710 cm^{-1} originates from the ester C═O stretching vibration of the PBT backbone. The absorption peak around 1 650 cm^{-1} indicates C═O stretching vibrations due to the amide Ⅰ band in APAP. These spectral changes suggest that NVA and AA are successfully grafted onto the PBT membrane through radiation grafting.

Figures 4(d) and 4(e) show the XPS spectra of the PBT-NVA-AA membrane (D_{gN} = 8%, D_{gA} = 15%). The PBT-NVA-AA membrane displays a nitrogen peak. The surface atomic percentages of C, N, and O are determined to be 70.01%, 5.04%, and 24.95%, respectively. In the fine spectrum of C1s, characteristic peaks corresponding to C—C, C—O, O═C—N—H, and O═C—O appear at binding energies of 284.80, 286.34, 287.89, and 288.78 eV, respectively. These features suggest that NVA and AA are successfully grafted onto the PBT membrane[30-31].



(a)



(b)

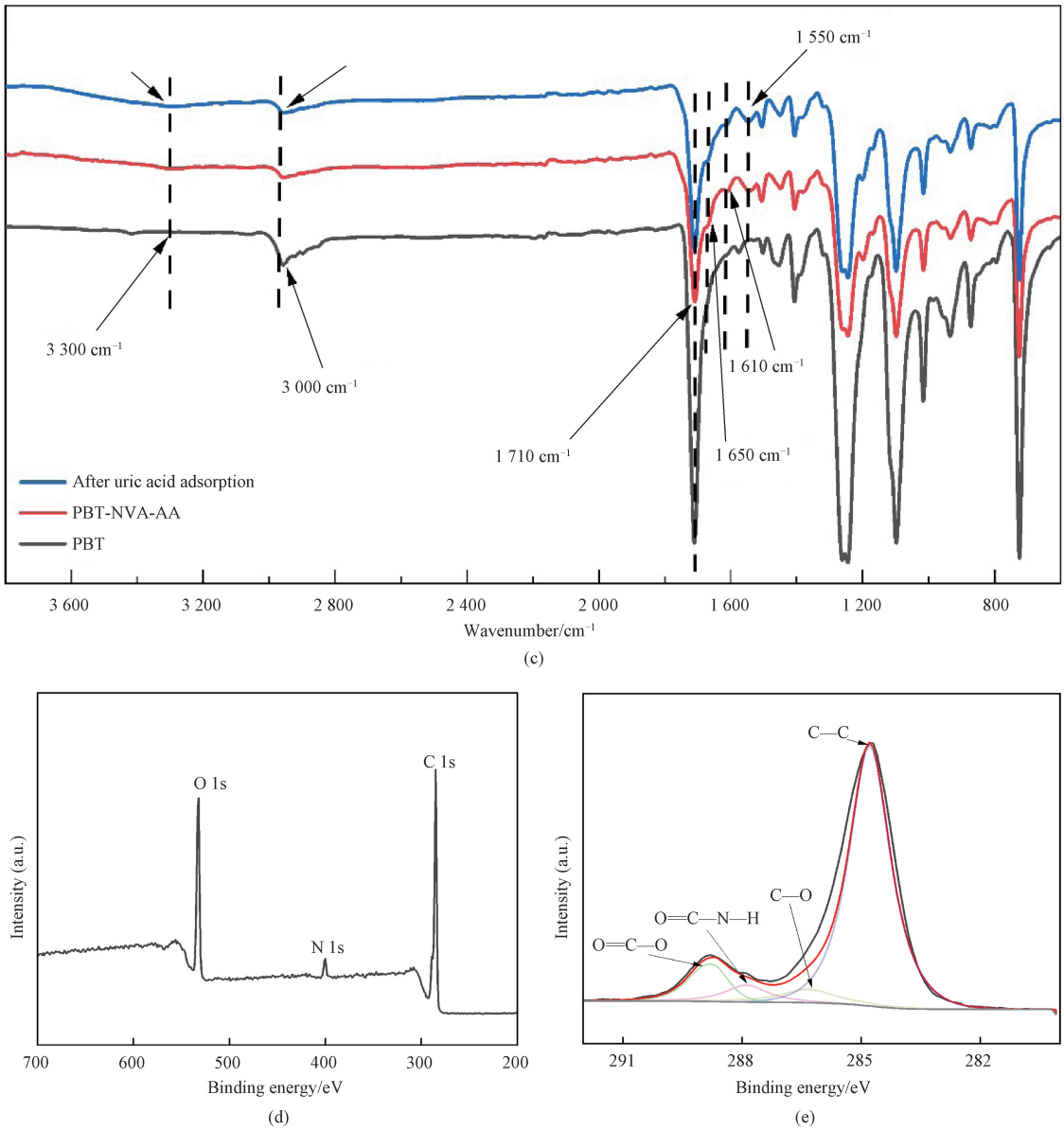


Fig. 4 Physicochemical characteristics of NVA, PBT, and PBT-NVA-AA membranes: (a) ^{1}H NMR of NVA; (b) HRMS of NVA; (c) FTIR of PBT and PBT-NVA-AA membranes; (d) XPS survey spectrum of PBT-NVA-AA membrane; (e) C 1s fine spectrum of PBT-NVA-AA membrane

2.2 Surface morphology of PBT-NVA-AA membrane

Scanning electron microscopy (SEM) was applied to observe the surface morphology of PBT and PBT-NVA-AA membranes. Figures 5(a) and 5(d) depict the smooth fiber surfaces of PBT, with no obvious cross-linking or particles between the fibers. Figures 5(b) and 5(e) display the morphology of the PBT-NVA-AA membrane with grafting degrees of D_{gN} = 4% and D_{gA} = 15%. The fiber surface resembles that of the original PBT, indicating that low grafting degrees have minimal impact on its surface morphology. Figures 5(c) and 5(f) display the PBT-NVA-AA membrane with grafting degrees of D_{gN} = 10% and D_{gA} = 15%. Noticeable particles appear on the fiber surface, and the morphology becomes rougher, which is consistent with the higher grafting degree. Additionally, Fig. 5(f) reveals complex cross-linked structures between adjacent fibers, which may be attributed to enhanced interfacial interactions after grafting. The increased surface particles and fiber crosslinking could provide more accessible sites, potentially contributing to the enhanced uric acid adsorption performance of the modified membrane.

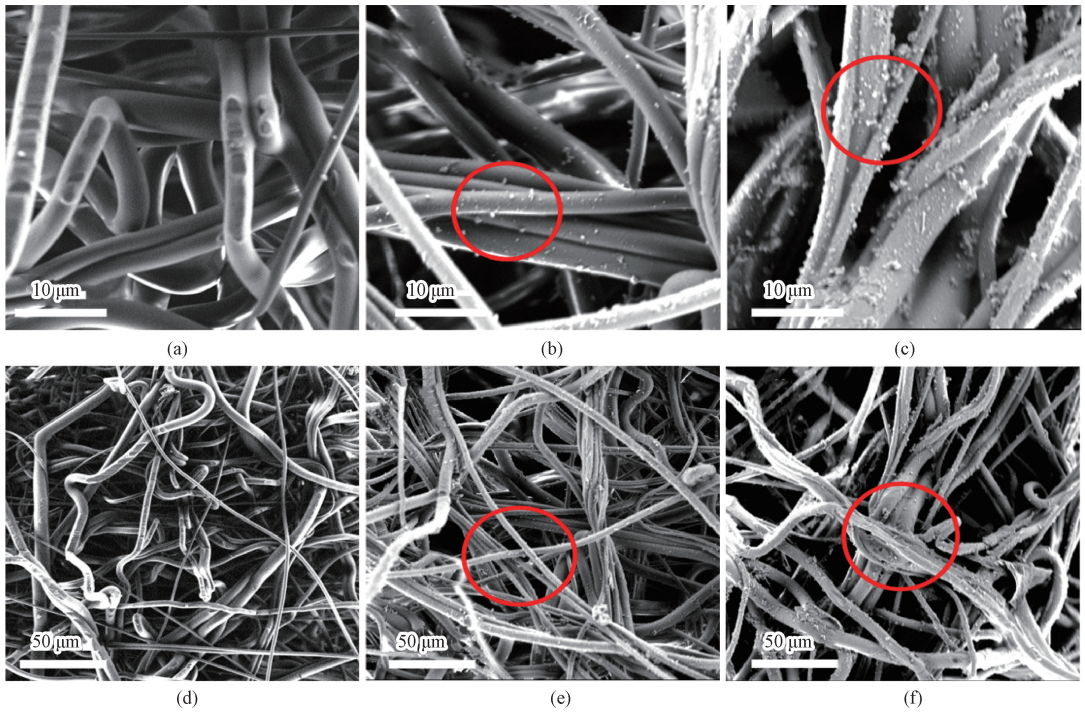


Fig. 5 SEM images of PBT and PBT-NVA-AA membranes: (a) and (d) PBT membrane; (b) and (e) PBT-NVA-AA membrane (D_{gN} = 4%, D_{gA} = 15%); (c) and (f) PBT-NVA-AA membrane (D_{gN} = 10%, D_{gA} = 15%)

2.3 Water contact angle and water absorption of PBT-NVA-AA membrane

Although the radiation grafting of NVA can enhance the membrane's uric acid adsorption performance, its strong hydrophobicity[32] limits the contact efficiency between the membrane and the uric acid solution. Therefore, to increase the membrane's hydrophilicity and biocompatibility[33-34], AA was introduced onto the PBT surface[35-37]. With AA grafting degree fixed, the variation in NVA content would still modulate the overall surface hydrophilicity of the composite membrane.

Figure 6 illustrates the effect of D_{gN} on the water contact angle and water absorption rate of the PBT-NVA-AA membrane at a constant D_{gA} of 15%.

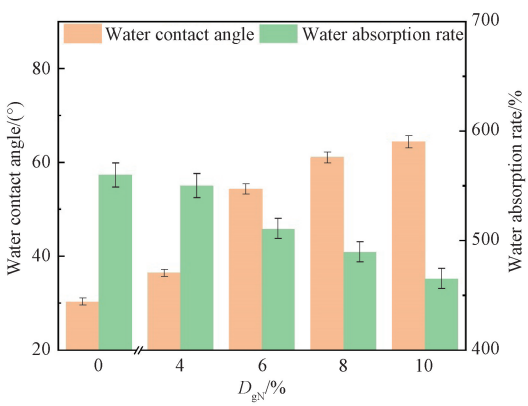


Fig. 6 Effect of D_{gN} on water contact angle and water absorption rate of PBT-NVA-AA membrane

When D_{gN} is 0 (corresponding to the PBT membrane grafted with AA only, without NVA), the membrane surface is relatively hydrophilic due to the —COOH group of AA grafted onto the PBT surface, resulting in a relatively low water contact angle. As D_{gN} increases, the introduction of hydrophobic groups leads to an increase in the water contact angle from (30.00±0.24)° to (64.41±0.35)° and a gradual decrease in water absorption rate from (560±18)% to (465±14)%.

2.4 Effect of D_{gA} and D_{gN} on uric acid adsorption

Figure 7(a) shows the effect of D_{gA} on uric acid adsorption of the PBT-NVA-AA membrane at a constant D_{gN} of 8%. It is observed that the uric acid adsorption rate first increases and then decreases as D_{gA} increases. The maximum adsorption rate of (5.46±0.12)% is achieved at a D_{gA} of 15%. The increase in D_{gA} introduces more —COOH groups onto the membrane surface, thereby providing more adsorption sites and consequently enhancing the uric acid adsorption performance. However, when D_{gA} increases from 15% to 20%, the adsorption rate decreases to (2.83±0.08)%. Excessive grafting may cause more crosslinks between fibers, hindering uric acid molecules from accessing adsorption sites, thereby reducing the adsorption rate. These results indicate that the optimal adsorption performance of the PBT-NVA-AA membrane is achieved at a D_{gA} of 15%.

The mechanism of uric acid adsorption on APAP[14-15] can be explained by the following factors. 1) APAP contains amide groups, which can interact with uric acid molecules via hydrogen bonding[23-24],

electrostatic forces[22], and van der Waals forces, leading to increased adsorption of uric acid. 2) Both APAP and uric acid molecules contain aromatic rings, which can enhance adsorption through π-π interactions[24]. 3) Grafting APAP may alter the surface area and pore structure of PBT. The increased surface area and appropriate pore structure facilitate uric acid adsorption by providing more adsorption sites, making it easier to capture uric acid molecules. These combined mechanisms enhance the material's uric acid adsorption performance.

Figure 7(b) illustrates the effect of D_{gN} on uric acid adsorption in both blood and aqueous solution at a constant D_{gA} of 15%. As shown in Fig. 7(b), the PBT-NVA-AA membrane exhibits a higher uric acid adsorption rate in the aqueous solution than in blood, which may be attributed to the complexity of the medium. Blood is a complex biological environment containing blood cells and other components that may inhibit the adsorption process, while the aqueous solution is simpler and less affected by external factors. During uric acid filtration in the blood, certain blood components may adhere to the membrane surface, forming an inhibitory layer that reduces uric acid adsorption. The uric acid adsorption rate increases slowly at lower grafting degrees of NVA, then increases quickly and attains a maximum value of (6.80±0.20)% at D_{gN} of 8%, but declines as the grafting degree increases further. This may be due to the hydrophobicity of APAP, which, while enhancing uric acid adsorption, reduces membrane hydrophilicity and weakens interfacial interactions, thereby increasing mass transfer resistance and decreasing adsorption. Additionally, elevated grafting degrees substantially reduce inter-fiber pore sizes. In consequence, the diffusion and transport pathways of uric acid molecules through the modified membrane are hindered, reducing effective uric acid adsorption.

To further evaluate the synergistic effect of NVA and AA grafting, a control experiment with AA grafting was conducted. The PBT-NVA membrane (grafted with NVA only) lacked hydrophilicity and, therefore, could not filter aqueous solution or blood, resulting in no uric acid adsorption. The PBT-AA membrane (grafted with AA only, represented as $D_{gN}=0$ in Fig. 7(b)) shows a uric acid adsorption rate of (0.10±0.02)% in blood. These results indicate a synergistic effect between the two monomers, with the combination of NVA and AA enhancing the adsorption performance.

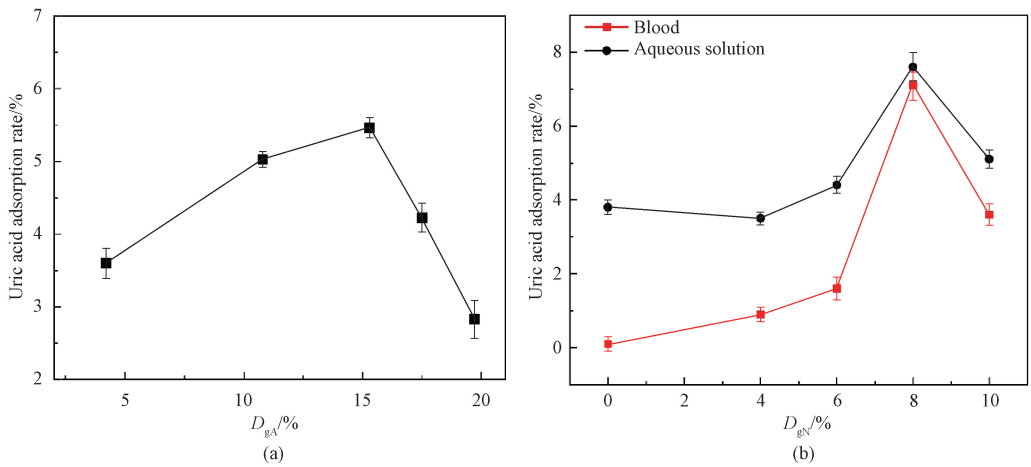


Fig. 7 Effect of D_{gA} and D_{gN} on uric acid adsorption rate: (a) effect of D_{gA} on uric acid adsorption rate in aqueous solution; (b) effect of D_{gN} on uric acid adsorption rate in blood and aqueous solution

2.5 Effect of uric acid concentration on adsorption performance

Figure 8 shows the uric acid adsorption rates of the PBT-NVA-AA membrane (D_{gN} = 8%, D_{gA} = 15%) at different uric acid concentrations. As the uric acid concentration increases from 200 μmol/L to 350 μmol/L, the adsorption rate increases from (6.50±0.10)% to (10.90±0.12)%. At low concentrations, the probability of uric acid molecules colliding with the membrane surface and occupying the active sites is lower, resulting in a lower adsorption rate.

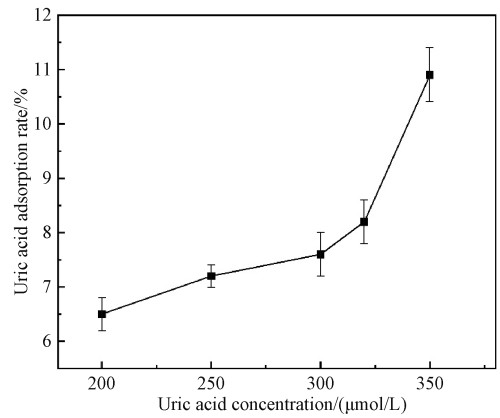


Fig. 8 Effect of uric acid concentration on adsorption rate

In contrast, as the uric acid concentration increases, the collision frequency between uric acid molecules and the membrane surface rises, and the mass transfer driving force becomes stronger. This facilitates more effective contact with the active adsorption sites on the membrane, thereby enhancing the adsorption performance. Uric acid exhibits relatively poor solubility in aqueous solution. According to Cheng et al.[38], the solubility of uric acid in the aqueous solution at 25 ℃ is approximately 360 μmol/L. When the concentration exceeds the saturation solubility, uric acid is prone to crystallization on the membrane. This phenomenon, known as crystallization adsorption[22-23], leads to the immobilization of uric acid on the membrane surface, further enhancing the overall adsorption performance.

2.6 Adsorption isotherm

The adsorption isotherm was tested using the PBT-NVA-AA membrane (D_{gN} = 8%, D_{gA} = 15%). The adsorption mechanism was explored using the Langmuir and the Freundlich models[39-40]. The Langmuir model assumes monolayer adsorption onto a surface with a finite number of identical adsorption sites. This model is appropriate when there is uniformity in the adsorption sites and no interactions between adsorbed molecules. The Freundlich model assumes multilayer adsorption and applies to surfaces with heterogeneous adsorption sites. It is used when adsorption occurs on irregular surfaces, where sites with varying affinities for the adsorbate are present. The parameters of the two adsorption isotherm models are shown in Table 1, and the Freundlich adsorption isotherm is shown in Fig. 9.

Table 1 Parameters of two adsorption isotherm models

Adsorption isotherm model	Parameter	Value
Langmuir	Q_m/(μmol/g)	4.89
	K_L	Negative
	R_1^2	0
Freundlich	K_F	2.17×10^{-5}
	n	0.33
	R_2^2	0.909

Note: R_1^2 and R_2^2 represent coefficients of determination for the Langmuir and Freundlich models, respectively.

The results show that the maximum adsorption capacity Q_m for the Langmuir model is 4.89 μmol/g, and the adsorption constant K_L is negative, with a coefficient of determination R_1^2 of 0, indicating that the model does not fit the data obtained. It is suggested that the material's adsorption behavior does not involve single-layer and uniform adsorption. The coefficient of determination R_2^2 of the Freundlich model is 0.909, with the Freundlich constant K_F of 2.17×10^{-5} and the adsorption intensity index n of 0.33. Given the limited experimental data points, this result tentatively suggests that the material's adsorption occurs on a heterogeneous surface, with uneven adsorption sites and relatively weak adsorption affinity. The Freundlich adsorption isotherm shown in Fig. 9 reveals that at low concentrations, the adsorption sites on the material are not fully utilized, but at high concentrations, adsorption increases gradually.

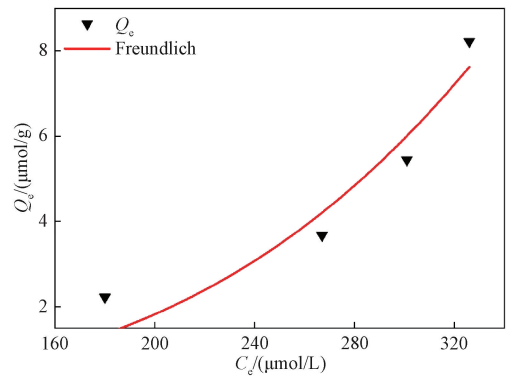


Fig. 9 Freundlich adsorption isotherm

2.7 Effect of PBT-NVA-AA membrane on blood cells

The surface chemical groups and hydrophilicity of the modified membrane are directly related to its performance in blood filtration[41-42]. The functional groups introduced during membrane radiation grafting not only change the surface energy but also influence protein adsorption behavior, which directly determines platelet adhesion and activation[43]. Previous studies[44-45] have demonstrated that membranes with higher hydrophilicity can reduce non-specific protein adsorption, effectively lowering platelet adhesion and activation. The membrane surface microstructure and the introduction of specific functional groups also play a regulatory role in leukocyte adhesion, affecting leukocyte interaction and activation by altering membrane-leukocyte interactions.

Figure 10 shows the effect of D_{gN} on blood cells after filtration through PBT-NVA-AA membranes. To assess the blood compatibility of the membrane, four blood cell count indices were compared. The differences in these indices reflect changes in blood cell counts after blood filtration, compared with untreated blood samples (control group, ck).

For the PBT-NVA-AA membrane with a grafting degree of D_{gN} = 0% and D_{gA} = 15% (denoted as M-a), the differences in red blood cell (RBC) count, platelet (PLT) count, and hematocrit (HCT) compared with the control group are relatively small. However, the white blood cell (WBC) count shows a larger difference (-1.31×10^9 L^{-1}), possibly due to the carboxyl groups on the membrane surface, which promote leukocyte adhesion[42]. For the PBT-NVA-AA membrane with a grafting degree of D_{gN} = 4% and D_{gA} = 15% (denoted as M-b), the differences in WBC count (-1.81×10^9 L^{-1}) and PLT count (-14.5×10^9 L^{-1}) suggest a more significant impact on leukocytes and platelets. NVA grafting likely contributed to increased leukocyte and PLT

adhesion by making the membrane surface more hydrophobic and rougher[19, 46-47]. For the PBT-NVA-AA membrane with a grafting degree of D_{gN} = 6% and D_{gA} = 15% (denoted as M-c), the difference in RBC count remains small. However, the differences in WBC count and PLT count further increase, showing a stronger effect at this grafting degree. For the PBT-NVA-AA membrane with a grafting degree of D_{gN} = 8% and D_{gA} = 15% (denoted as M-d), the differences in RBC count and HCT are relatively small. The WBC count difference is only 0.52 × 10^9 L^{-1}, indicating the closest match to the untreated blood data. It suggests that this grafting degree provides the best blood compatibility, possibly due to the membrane's moderate hydrophilicity, which controls protein adsorption and reduces platelet activation and leukocyte adhesion[19, 48-49]. For the PBT-NVA-AA membrane with a grafting degree of D_{gN} = 10% and D_{gA} = 15% (denoted as M-e), most blood cell indicators show minor deviations from the control, and it achieves the lowest PLT loss. Nevertheless, its overall comprehensive blood compatibility is inferior to M-d. Excessively high grafting increases surface hydrophobicity and fiber crosslinking, strengthening interactions between the membrane and leukocytes[50-51].

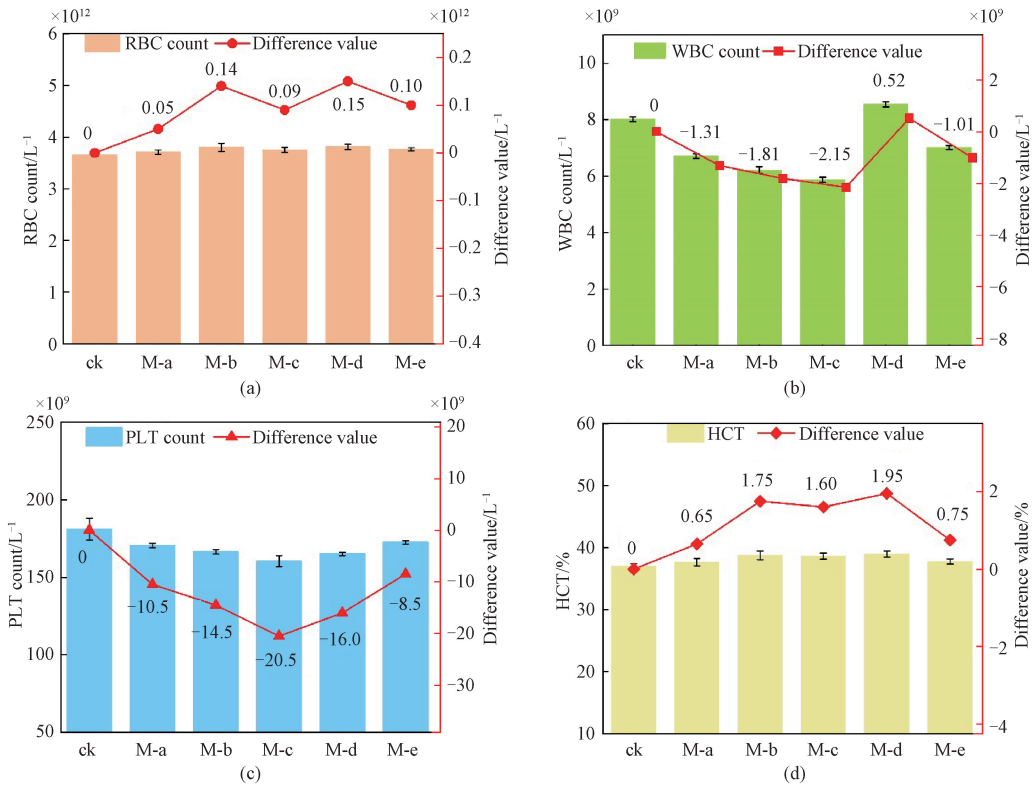


Fig. 10 Effect of PBT-NVA-AA membrane on blood cells: (a) RBC count; (b) WBC count; (c) PLT count; (d) HCT

Based on the blood compatibility analysis, M-d exhibits the optimal overall performance, particularly in maintaining the WBC count close to that of the control group. The results highlight significant differences between modified membranes in their impact on blood components, particularly on WBC and PLT counts. These findings provide valuable insights for the design of biomaterials with improved blood compatibility.

3 Conclusions

A modified PBT membrane biomaterial with the capability of uric acid adsorption and acceptable blood compatibility was prepared by radiation grafting with NVA and AA. This novel biomaterial holds great promise for blood purification, offering a potential solution to the limitations of current therapeutic approaches for gout and hyperuricemia. FTIR and XPS analyses confirmed the successful grafting of NVA and AA onto the PBT membrane surface. The introduction of these functional groups improved both the adsorption capacity and blood compatibility of the membrane. The PBT-NVA-AA membrane exhibited the optimal uric acid adsorption performance at D_{gN} = 8% and D_{gA} = 15%, achieving a blood uric acid adsorption rate of (6.80±0.20)%. This optimized PBT-NVA-AA membrane showed minimal impact on the blood cell counts, demonstrating good blood compatibility. This research provides a foundation for the further development of novel biomaterials with high efficiency and safety for clinical applications. Future studies should focus on improving the surface properties of the material, such as enhancing surface uniformity and increasing the number of active sites, to further optimize the adsorption performance.

Despite these promising results, the PBT-NVA-AA membrane still faces many challenges in blood purification applications. Future work should prepare a filter suitable for blood purification by combining materials, conduct blood circulation experiments using purification equipment, and examine issues such as material uniformity, cell adhesion, and activation caused by prolonged blood contact. Thus, the adsorption efficiency and blood compatibility of the membrane under continuous blood flow can be more accurately evaluated, and its clinical feasibility can be verified.

References

[1] Li D L, Yuan S Y, Deng Y Y, et al. The dysregulation of immune cells induced by uric acid: mechanisms of inflammation associated with hyperuricemia and its complications [J]. *Frontiers in Immunology*, 2023, 14: 1282890.

[2] El Ridi R, Tallima H. Physiological functions and pathogenic potential of uric acid: a review [J]. *Journal of Advanced Research*, 2017, 8(5): 487-493.

[3] Freilich M, Arredondo A, Zonnoor S L, et al. Elevated serum uric acid and cardiovascular disease: a review and potential therapeutic interventions [J]. *Cureus*, 2022, 14(3): e23582.

[4] Dalbeth N, Te Karu L, Stamp L K. Gout and its management [J]. *Internal Medicine Journal*, 2024, 54(5): 716-723.

[5] Shi C, Zhou Z T, Chi X W, et al. Recent advances in gout drugs[J]. *European Journal of Medicinal Chemistry*, 2023, 245: 114890.

[6] Pillinger M H, Mandell B F. Therapeutic approaches in the treatment of gout[J]. *Seminars in Arthritis and Rheumatism*, 2020, 50(3): S24-S30.

[7] Ma L K, Huang L L, Zhang Y Z, et al. Hemocompatible poly(lactic acid) membranes prepared by immobilizing carboxylated graphene oxide via mussel-inspired method for hemodialysis[J]. *RSC Advances*, 2018, 8(1): 153-161.

[8] Verma S K, Modi A, Singh A K, et al. Improved hemodialysis with hemocompatible polyethersulfone hollow fiber membranes: in vitro performance [J]. *Journal of Biomedical Materials Research Part B: Applied Biomaterials*, 2018, 106(3): 1286-1298.

[9] Ter Beek O, Pavlenko D, Suck M, et al. New membranes based on polyethersulfone-SlipSkin™ polymer blends with low fouling and high blood compatibility [J]. *Separation and Purification Technology*, 2019, 225: 60-73.

[10] Zhong D L, Wang Z G, Zhou J M, et al. Additive-free preparation of hemodialysis membranes from block copolymers of polysulfone and polyethylene glycol [J]. *Journal of Membrane Science*, 2021, 618: 118690.

[11] Wang H, Li J L, Liu F, et al. Enhanced hemocompatibility of flat and hollow fiber membranes via a heparin free surface crosslinking strategy[J]. *Reactive and Functional Polymers*, 2018, 124: 104-114.

[12] Gérard E, Bessy E, Hénard G, et al. Surface modification of poly(butylene terephthalate) nonwoven by photochemistry and biofunctionalization with peptides for blood filtration[J]. *Journal of Polymer Science Part A: Polymer Chemistry*, 2011, 49(23): 5087-5099.

[13] Cao Y, Wang H, Yang C, et al. In vitro studies of PBT nonwoven fabrics adsorbent for the removal of low density lipoprotein from hyperlipemia plasma [J]. *Applied Surface Science*, 2011, 257(17): 7521-7528.

[14] Zhao J, Shi Q, Luan S F, et al. Improved biocompatibility and antifouling property of polypropylene non-woven fabric membrane by surface grafting zwitterionic polymer[J]. *Journal of Membrane Science*, 2011, 369(1/2): 5-12.

[15] Hao T T, Niu G L, Zhang H, et al. Enhanced hemocompatibility and antibacterial activity of biodegradable poly(ester-urethane) modified with quercetin and phosphorylcholine for durable blood-contacting applications [J]. *Journal of Materials Chemistry B*, 2023, 11(25): 5846-5855.

[16] Iftikhar M, Othman M H D, Khan I U, et al. Future research perspectives in hemodialysis membrane technology[J]. *Journal of Industrial and Engineering Chemistry*, 2024, 138: 72-103.

[17] Rodríguez-Alba E, Dionisio N, Pérez-Calixto M, et al. Surface modification of polyethylenterephthalate film with primary amines using gamma radiation and aminolysis reaction for cell adhesion studies[J]. *Radiation Physics and Chemistry*, 2020, 176: 109070.

[18] Aarya S, Kumar P, Bhatia M, et al. Gamma rays induced modification in ultrahigh molecular weight polyethylene (UHMWPE)[J]. *Advances in Polymer Technology*, 2021, 2021(1): 7013154.

[19] Zhong R, He Z, Zhang X J, et al. The strategy of modulation blood responses by surface modification with different functional groups on polyester film [J]. *Journal of Biomedical Materials Research Part A*, 2021, 109(10): 1955-1966.

[20] Heller M, Wimbish R, Gurgel P V, et al. Reducing diffusion limitations in ion exchange grafted membranes using high surface area nonwovens[J]. *Journal of Membrane Science*, 2016, 514: 53-64.

[21] Salvagnini C, Roback A, Momtaz M, et al. Surface functionalization of a poly (butylene terephthalate) (PBT) melt-blown filtration membrane by wet chemistry and photo-grafting [J]. *Journal of Biomaterials Science, Polymer Edition*, 2007, 18(12): 1491-1516.

[22] Zhang C L, Xiao Z G, Qin T T, et al. Mechanism and kinetics of uric acid adsorption on nanosized hydroxyapatite coating[J]. *Journal of Saudi Chemical Society*, 2019, 23(2): 249-253.

[23] Kameda T, Horikoshi K, Kumagai S, et al. Adsorption of urea, creatinine, and uric acid onto spherical activated carbon [J]. *Separation and Purification Technology*, 2020, 237: 116367.

[24] El Saied M, Shaban S A, Mostafa M S, et al. Efficient adsorption of acetaminophen from the aqueous phase using low-cost and renewable adsorbent derived from orange peels[J]. *Biomass Conversion and Biorefinery*, 2024, 14(2): 2155-2172.

[25] Zhao L N, Liu F R, Li M, et al. Optimization of benorilate synthesis process [J]. *Shandong Chemical Industry*, 2024, 53(14): 33-37. (in Chinese)

[26] Chen Y F. Research on the preparation of methacryloyl chloride [J]. *Chemical Intermediates*, 2009 (1): 63-64. (in Chinese)

[27] Liang F, Chen Q X, Shi Z, et al. Multifunctional composites made from waste polyester cotton fabric and waste rigid polyurethane foam for potential building wall material applications[J]. *Energy and Buildings*, 2025, 329: 115274.

[28] Liang H, Shi Z, Dan R, et al. Waste-wool/polyurethane foam composites with stratified structure for potential sound absorption applications [J]. *Journal of Building Engineering*, 2024, 98: 111238.

[29] Chen Q X, Shi Z, Dan R, et al. Preparation and characterization of waste cotton fabric reinforced polylactic acid green composites with multifunctional properties in a low-carbon process [J]. *Process Safety and Environmental Protection*, 2024, 192: 412-423.

[30] Zhang W, Li J X, Tang R C, et al. Hydrophilic and antibacterial surface functionalization of polyamide fabric by coating with polylysine biomolecule[J]. *Progress in Organic Coatings*, 2020, 142: 105571.

[31] Cao Y, Liu J X, Zhong R, et al. Surface modification of PBT nonwoven fabrics used for blood filtration and their blood compatibility study [J]. *Artificial Cells, Blood Substitutes, and Biotechnology*, 2012, 40(5): 317-325.

[32] Miao X Y, Shi Z, Dan R, et al. Research on the application of a PET/PP composite board prepared by recycling waste polyester clothing in furniture products[J]. *ACS Sustainable Resource Management*, 2024, 1(5): 890-897.

[33] Zhang Y H, Zhang M L, Xu X, et al. Anti-fouling surfaces for extracorporeal membrane oxygenation by surface grafting of hydrophilic sulfoxide polymers [J]. *Biomacromolecules*, 2022, 23(10): 4318-4326.

[34] Ji M B, Chen X R, Luo J Q, et al. Improved blood compatibility of polysulfone membrane by anticoagulant protein immobilization [J]. *Colloids and Surfaces B: Biointerfaces*, 2019, 175: 586-595.

[35] Abd Ghani F, Hamzah K, Mohamed N H. Modification of PTFE flat sheet film via radiation induced grafting polymerization with acrylic acid [J]. *Sains Malaysiana*, 2020, 49(1): 169-178.

[36] Chen F E, Xie L. Enhanced fouling-resistance performance of polypropylene hollow fiber membrane fabricated by ultrasonic-assisted graft polymerization of acrylic acid [J]. *Applied Surface Science*, 2020, 502: 144098.

[37] Shen L G, Zhang Y C, Yu W M, et al. Fabrication of hydrophilic and antibacterial poly (vinylidene fluoride) based separation membranes by a novel strategy combining radiation grafting of poly(acrylic acid) (PAA) and electroless nickel plating [J]. *Journal of Colloid and Interface Science*, 2019, 543: 64-75.

[38] Cheng L, Zhang J L. Determination of solubility of uric acid and purine in water and phosphate buffer[J]. *Food and Nutrition in China*, 2014, 20(11): 67-69. (in Chinese)

[39] Wang G L, Li G F, Huan Y Y, et al. Acrylic acid functionalized graphene oxide: high-efficient removal of cationic dyes from wastewater and exploration on adsorption mechanism [J]. *Chemosphere*, 2020, 261: 127736.

[40] Sumalinog D A G, Capareda S C, De Luna M D G. Evaluation of the effectiveness and mechanisms of acetaminophen and methylene blue dye adsorption on activated biochar derived from municipal solid wastes [J]. *Journal of Environmental Management*, 2018, 210: 255-262.

[41] Sperling C, Schweiss R B, Streller U, et al. In vitro hemocompatibility of self-assembled monolayers displaying various functional groups [J]. *Biomaterials*, 2005, 26(33): 6547-6557.

[42] Barbosa J N, Barbosa M A, Águas A P. Adhesion of human leukocytes to biomaterials: an in vitro study using alkanethiolate monolayers with different chemically functionalized surfaces [J]. *Journal of Biomedical Materials Research Part A*, 2003, 65A(4): 429-434.

[43] Tsai M Y, Lin J C. Surface characterization and platelet adhesion studies of self-assembled monolayer with phosphonate ester and phosphonic acid functionalities [J]. *Journal of Biomedical*

Materials Research, 2001, 55(4): 554-565.
[44] Özgüzar H F, Evren E, Meydan A E, et al. Plasma-assisted surface modification and heparin immobilization: dual-functionalized blood-contacting biomaterials with improved hemocompatibility and antibacterial features[J]. *Advanced Materials Interfaces*, 2023, 10(6): 2202009.
[45] Bhattacharjee A, Savargaonkar A V, Tahir M, et al. Surface modification strategies for improved hemocompatibility of polymeric materials: a comprehensive review[J]. *RSC Advances*, 2024, 14(11): 7440-7458.
[46] Merkle V M, Martin D, Hutchinson M, et al. Hemocompatibility of poly(vinyl alcohol)-gelatin core-shell electrospun nanofibers: a scaffold for modulating platelet deposition and activation[J]. *ACS Applied Materials & Interfaces*, 2015, 7(15): 8302-8312.
[47] Moradi S, Hadjesfandiari N, Toosi S F, et al. Effect of extreme wettability on platelet adhesion on metallic implants: from superhydrophilicity to superhydrophobicity[J]. *ACS Applied Materials & Interfaces*, 2016, 8(27): 17631-17641.
[48] Ishihara K, Fukumoto K, Iwasaki Y, et al. Modification of polysulfone with phospholipid polymer for improvement of the blood compatibility: part 2: protein adsorption and platelet adhesion[J]. *Biomaterials*, 1999, 20(17): 1553-1559.
[49] Tanaka M, Motomura T, Kawada M, et al. Blood compatible aspects of poly(2-methoxyethylacrylate)(PMEA): relationship between protein adsorption and platelet adhesion on PMEA surface[J]. *Biomaterials*, 2000, 21(14): 1471-1481.
[50] Park A, Song Y J, Yi E, et al. Blood oxygenation using fluoropolymer-based artificial lung membranes[J]. *ACS Biomaterials Science & Engineering*, 2020, 6(11): 6424-6434.
[51] Xu Z H, Hwang D G, Bartlett M D, et al. Alter macrophage adhesion and modulate their response on hydrophobically modified hydrogels[J]. *Biochemical Engineering Journal*, 2021, 165: 107821.

辐射接枝制备 PBT 生物材料用于增强尿酸吸附和血液相容性

莫耀翔[1], 李　淳[1], 王斯琦[1], 薛嘉贺[1], 沈　丽[1], 王衡东[2*], 陈前进[1*]
1. 东华大学 化学与化工学院, 上海 201620
2. 中国科学院上海应用物理研究所, 上海 201821

摘　要: 通过血液净化有效去除血液中的尿酸是治疗痛风和高尿酸血症的一种新方法。本研究通过辐射接枝 *N*-(4-乙烯基甲酰氧基苯基)乙酰胺和丙烯酸，制备了一种具有较好尿酸吸附性能和良好血液相容性的新型聚对苯二甲酸丁二酯(polybutylene terephthalate, PBT)生物膜材料。通过傅里叶变换红外光谱、X 射线光电子能谱和扫描电子显微镜研究了改性膜材料的化学结构和表面形貌。通过测定水接触角和吸水率来评价其亲水性。结果表明，改性膜材料的最大血液尿酸吸附率为(6.80±0.20)%，且对血液细胞计数影响最小。本研究为开发用于痛风及高尿酸血症治疗的高效、安全生物膜材料提供了一种具有应用前景的思路。

关键词: 尿酸吸附; 辐射接枝; 聚对苯二甲酸丁二酯 (PBT); *N*-(4-乙烯基甲酰氧基苯基)乙酰胺; 血液细胞计数